European Journal of Medicinal Chemistry 123 (2016) 298–308

Contents lists available at ScienceDirect

European Journal of Medicinal Chemistry

journal homepage: http://www.elsevier.com/locate/ejmech

Research paper

Synthesis and structure-activity relationship study of tacrine-based pyrano[2,3-*c*]pyrazoles targeting AChE/BuChE and 15-LOX

Ladan Pourabdi [a], Mehdi Khoobi [b, c], Hamid Nadri [d], Alireza Moradi [d], Farshad Homayouni Moghadam [e], Saeed Emami [f], Mohammad M. Mojtahedi [a, **], Ismaeil Haririan [b], Hamid Forootanfar [g], Alieh Ameri [h], Alireza Foroumadi [c], Abbas Shafiee [c, *]

[a] Department of Organic Chemistry and Natural Products, Chemistry and Chemical Engineering Research Center of Iran, Pajohesh Blvrd., 17th Km of Tehran Karaj Highway, P.O. Box 14335-186, Tehran, Iran
[b] Department of Pharmaceutical Biomaterials and Medical Biomaterials Research Center, Faculty of Pharmacy, Tehran University of Medical Sciences, Tehran, Iran
[c] Department of Medicinal Chemistry, Faculty of Pharmacy and Pharmaceutical Sciences Research Center, Tehran University of Medical Sciences, Tehran 14176, Iran
[d] Department of Medicinal Chemistry, Faculty of Pharmacy, Shahid Sadoughi University of Medical Sciences, Yazd, Iran
[e] Department of Cellular Biotechnology, Cell Science Research Center, Royan Institute for Biotechnology, ACECR, Isfahan, Iran
[f] Department of Medicinal Chemistry and Pharmaceutical Sciences Research Center, Faculty of Pharmacy, Mazandaran University of Medical Sciences, Sari, Iran
[g] Pharmaceutics Research Center, Institute of Neuropharmacology, Kerman University of Medical Sciences, Kerman, Iran
[h] Department of Medicinal Chemistry, Faculty of Pharmacy, Kerman University of Medical Sciences, Kerman, Iran

ARTICLE INFO

Article history:
Received 17 February 2016
Received in revised form
28 May 2016
Accepted 20 July 2016
Available online 21 July 2016

Keywords:
Acetylcholinesterase
Butyrylcholinesterase
15-Lipoxygenase
Alzheimer's disease
Tacrine

ABSTRACT

A series of tacrine-based pyrazolo[4′,3′:5,6]pyrano[2,3-*b*]quinolines and related compounds were designed and synthesized for targeting AChE, BuChE and 15-LOX enzymes in the field of Alzheimer's disease therapy. Most of compounds showed potent activity against cholinesterases and mild potency toward 15-LOX enzyme. In particular, compounds **29**, **32** and **40** displayed inhibition at nano-molar level against AChE and BuChE (IC_{50}s = 0.005–0.08 μM), being more potent than reference drug tacrine. Moreover, compound **32** with IC_{50} value of 31 μM was the most potent compound against 15-LOX. The cytotoxicity assay on HepG2 cells revealed that compounds **29** and **32** showed no significant cytotoxic activity even at concentration of 50 μM. The cytotoxicity of compounds **29** and **32** was significantly less than that of tacrine at higher concentrations.

1. Introduction

Alzheimer's disease (AD) is the most common form of dementia that affects elderly people, resulting in loss of memory, learning and cognitive functions [1]. It is estimated that there are about 35 million people suffering from AD worldwide. Due to the increase of average age of the population, it also predicted that the incidence of AD is significantly rose to 66 million by 2030 [2,3]. This neurodegenerative disease is characterized by an irreversible degeneration of cholinergic neurons in the central nervous system [4]. The decline in the cholinergic function of the brain results in the loss of memory and cognitive functions which is usually accompanied by behavioral disturbances [5]. The cholinergic hypothesis of memory dysfunction in patient with AD is the basis for treating this disease [6]. In particular, the main approach in the AD treatment is the improvement of cholinergic neurotransmission by inhibiting acetylcholinesterase (AChE) and butyrylcholinesterase (BuChE). By increasing the levels of acetylcholine (ACh) in the brain through inhibition of these enzymes, it is possible to reducing cognitive decline but not allowing the recovery or stopping the progression of the disease [7,8].

AD is a complicated disease with different molecular events,

* Corresponding author.
** Corresponding author.
E-mail address: ashafiee@ams.ac.ir (A. Shafiee).

http://dx.doi.org/10.1016/j.ejmech.2016.07.043
0223-5234/

which could be better managed by agents acting upon more than one target [1]. Besides cholinergic hypothesis, several evidences suggest that oxidative stress could play a functional role in the pathogenesis of AD. In particular, recent works have highlighted that the 12/15-lipoxygenase (12/15-LOX) metabolic pathways may contribute to the pathogenesis of this neurodegenerative disorder [9,10]. The LOX enzymes catalyze the oxidation of poly-unsaturated fatty acids such as arachidonic acid to hydroperoxy acids, which are potent pro-oxidant mediators [11,12]. Accordingly, the 12/15-LOX could be considered as an emerging therapeutic target for AD.

Tacrine, an aminoacridine derivative is a reversible inhibitor of AChE and BuChE. This compound is the first drug that was approved by the Food and Drug Administration of United States of America for clinical use in the treatment of AD. Tacrine was found to be hepatotoxic and soon withdrawn from the market [13,14]. Thus the modification of tacrine core structure was frequently used to find new compounds with high anti-cholinesterase potency and acceptable safety. Several modifications concern benzene ring in tacrine by replacing or annulating with different heterocyclic systems. For example numerous tacrine analogs, such as coumarin [15], pyrazolo[3,4-*b*]quinoline and benzo[*b*]pyrazolo[4,3-*g*] [1,8] naphthyridine [16], and benzochromene [17,18] derivatives have been reported as multi-targeted AChE inhibitors with regard to Alzheimer's disease treatment. Furthermore, several multi-target tacrine-coumarin and tacrine-trolox hybrids have been described for the treatment of Alzheimer's disease [19,20].

Recently, we designed a series of tacrine-based compounds **I** (Fig. 1) by replacing the benzene ring of tacrine with aryl-dihydropyrano[2,3-*c*]pyrazole [21]. The in vitro biological evaluation of target compounds **I** showed that most of them had potent inhibitory activity against AChE at sub-micromolar range. The 3,4-dimethoxyphenyl derivative (Ar = 3,4-$(OMe)_2$Ph) was the potent compound, being more active than reference drug tacrine. Also, this compound could significantly protect neurons against oxidative stress. In continuation of our work, we focused on the structure-activity relationship study of tacrine analogs bearing aryl-dihydropyrano[2,3-*c*]pyrazole scaffold, by modification of core structure and side chains. Thus we report here, the preparation of new tacrine-based compounds **II** (Fig. 1) and evaluation of their inhibitory activity against AChE, BuChE and 15-LOX.

2. Chemistry

The target compounds **9**–**40** were synthesized utilizing an efficient route as illustrated in Scheme 1. The intermediates **5**–**7** were synthesized via one-pot four-component reaction of β-ketoester **1**, hydrazine derivative **2**, malononitrile (**3**) and appropriate aldehyde **4** in the presence of (*S*)-proline in aqueous media under ultrasonic irradiation for 10–30 min (Table 1) [21]. The cyclocondensation of the obtained pyrano[2,3-*c*]pyrazoles **5**–**7** and cyclic ketone **8** in the presence of $AlCl_3$ in dry 1,2-dichloroethane under reflux gave final compounds **9**–**40**. The results are given in Table 2. It should be noted that the pyranopyridines **9**–**40** were exclusively isolated in the reaction condition with no detectable byproducts.

3. Results and discussion

3.1. AChE inhibitory activity

The inhibitory activity of target compounds was evaluated in vitro against AChE and the obtained IC_{50} values were presented in Table 3. The results revealed that most tested compounds had remarkable anti-AChE activity (IC_{50} values < 2 μM). In particular, 3-propyl derivatives **10**, **16**, **19**, **20**, 3-phenyl derivatives **28**, **29**, **31**, **32**, **36**, and 3-(furan-2-yl) analogs **39**, and **40** showed comparable or superior activity respect to the reference drug tacrine. Among them, compound **29** with IC_{50} value of 0.034 μM was 6-fold more potent than tacrine. From a SAR point of view, compounds bearing R_1 = Pr or Ph and R_3 = 4-MeO-Ph or 4-F-Ph showed the best inhibitory activity against AChE. The effect of ring expansion (alteration of X = CH_2 to X = CH_2CH_2) depended on the type of substituents. For example, ring expansion in compound **10** resulted in compound **25** with diminished activity. In contrast, the cycloheptane analog **36** was more active than compound **28** containing six-membered ring. The comparison of compounds possessing X = S with X = CH_2 revealed that bioisoesteric replacement of CH_2 by S could not improve the AChE inhibitory activity. While the *N*-phenylpyrazole analog **35** showed no activity against AChE but *N*-phenylpyrazole derivative **40** bearing R_1 = 2-furyl moiety was a potent compound. The presence of isopropyl group (compound **34**) instead of aryl moiety at R_3 had negative effect on the anticholinesterase activity. In the compounds with phenyl moiety at R_3, the presence of 4-methoxy group on the phenyl ring was favorable for inhibitory activity. However, introduction of additional methoxy groups (3,4-dimethoxy or 3,4,5-trimethoxy patterns) led to decrease of the activity against AChE. These findings demonstrated that introduction of suitable substituents at R_1, R_2 and R_3 can modulate the anti-AChE activity of the basic structure.

3.2. BuChE inhibitory activity

The in vitro effect of target compounds toward BuChE was similarly evaluated and the results were listed in Table 3 as IC_{50} values (μM). All tested compounds with the exception of tri-phenyl derivative **35** (R_1 = R_2 = R_3 = Ph) showed potent activity against BuChE (IC_{50} values ≤ 0.570 μM). Among them, compounds **10**, **19**, **20**, **28**, **29**, **32**, **36**, and **40** were more potent than tacrine. The 2-furyl derivative **40** (R_1 = 2-furyl) with IC_{50} value of 0.005 μM was the most potent compound against BuChE. In the propyl series (compounds **9**–**27**, R_1 = Pr), the 4-methoxyphenyl derivative **19** found to be the most potent compound (IC_{50} = 0.006 μM). In the case of phenyl derivatives (**28**–**38**, R_1 = Ph), compounds **29** and **32** (4-fluorophenyl and 4-methoxyphenyl derivatives, respectively) showed superior activity against BuChE. The replacement of X = CH_2 with X = CH_2CH_2 or S had no favorable effect on inhibitory activity.

As observed in Table 3, the IC_{50} values of compound **9**–**40** as well as reference drug tacrine against BuChE were significantly less than those against AChE. The selectivity indexes (SIs) for BuChE over AChE were in the range of 4.0–35.3. The highest selectivity for

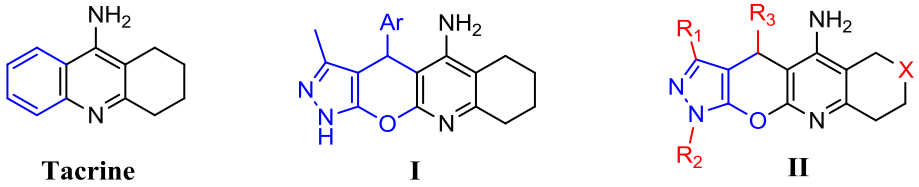

Fig. 1. Structures of tacrine and tacrine-derived compounds **I** and **II**.

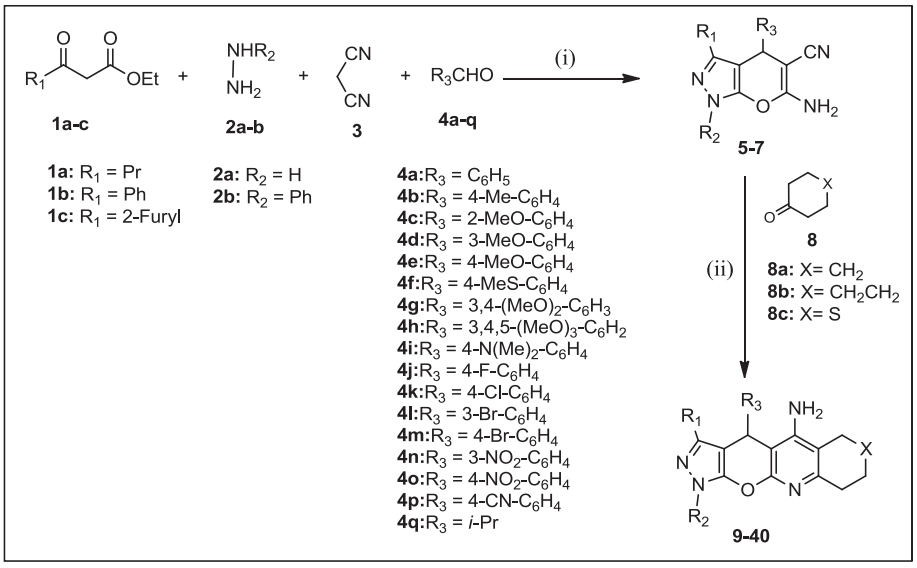

Scheme 1. Synthetic route to compounds **9**–**40**. Reagents and conditions: (i) (*S*)-proline (10% mol), water, ultrasonic irradiation, 10–30 min; (ii) $AlCl_3$ (1.5 equiv.), dry 1,2-dichloroethane, reflux, 24 h.

BuChE was observed with compound **13**. Notably, the promising anticholinesterase (compound **29**) showed low selectivity (SI= IC_{50} AChE/IC_{50} BuChE = 4.9).

3.3. 15-LOX inhibitory activity

All title compounds **9**–**40** were tested against 15-LOX enzyme and the obtained results were shown in Table 3. All compounds with the exception of **29**, **30** and **35** exhibited mild activity against

Table 1
The substrates, products and yields in the synthesis of pyrano[2,3-*c*]pyrazoles **5**–**7**.

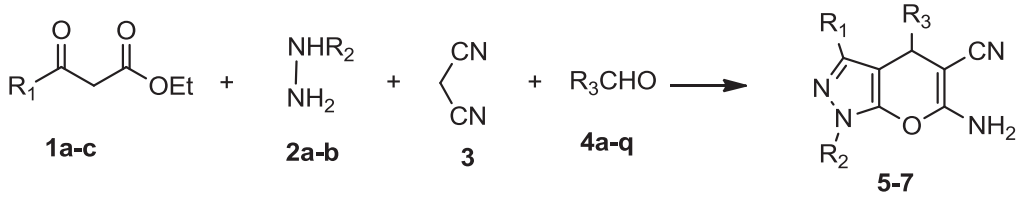

Entry	Ethyl β-ketoester	Hydrazine	Aldehyde	Product	Yield (%)[a]
1	**1a**	**2a**	**4a**	**5a**	94
2	**1a**	**2a**	**4b**	**5b**	87
3	**1a**	**2a**	**4c**	**5c**	90
4	**1a**	**2a**	**4d**	**5d**	95
5	**1a**	**2a**	**4e**	**5e**	93
6	**1a**	**2a**	**4f**	**5f**	86
7	**1a**	**2a**	**4g**	**5g**	89
8	**1a**	**2a**	**4h**	**5h**	91
9	**1a**	**2a**	**4i**	**5i**	79
10	**1a**	**2a**	**4k**	**5j**	88
11	**1a**	**2a**	**4l**	**5k**	90
12	**1a**	**2a**	**4m**	**5l**	92
13	**1a**	**2a**	**4n**	**5m**	93
14	**1a**	**2a**	**4o**	**5n**	91
15	**1a**	**2a**	**4p**	**5o**	89
16	**1b**	**2a**	**4a**	**6a**	87
17	**1b**	**2a**	**4b**	**6b**	81
18	**1b**	**2a**	**4e**	**6c**	83
19	**1b**	**2a**	**4h**	**6d**	80
20	**1b**	**2a**	**4j**	**6e**	92
21	**1b**	**2a**	**4k**	**6f**	90
22	**1b**	**2a**	**4q**	**6g**	79
23	**1b**	**2b**	**4a**	**6h**	77
24	**1c**	**2a**	**4a**	**7a**	91
25	**1c**	**2b**	**4a**	**7b**	84

[a] Isolated yield.

Table 2
Synthesis of compounds **9**–**40**.

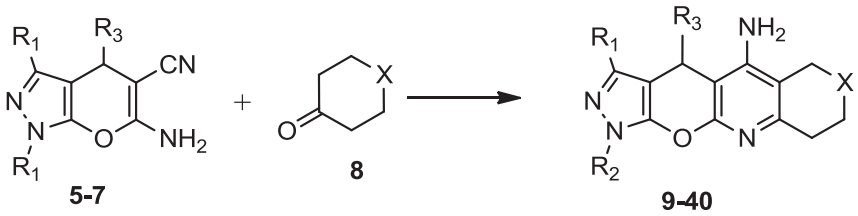

Entry	6-Amino-2,4-dihydropyrano [2,3-*c*]pyrazole (**5**–**7**)	Cyclic ketone (**8**)	Product	Yield (%)[a]
1	**5a**	**8a**	**9**	87
2	**5j**	**8a**	**10**	93
3	**5k**	**8a**	**11**	87
4	**5l**	**8a**	**12**	92
5	**5m**	**8a**	**13**	90
6	**5n**	**8a**	**14**	93
7	**5o**	**8a**	**15**	84
8	**5b**	**8a**	**16**	89
9	**5c**	**8a**	**17**	82
10	**5d**	**8a**	**18**	84
11	**5e**	**8a**	**19**	88
12	**5f**	**8a**	**20**	85
13	**5g**	**8a**	**21**	89
14	**5h**	**8a**	**22**	87
15	**5i**	**8a**	**23**	81
16	**5a**	**8b**	**24**	85
17	**5j**	**8b**	**25**	86
18	**5j**	**8c**	**26**	89
19	**5b**	**8c**	**27**	86
20	**6a**	**8a**	**28**	92
21	**6e**	**8a**	**29**	94
22	**6f**	**8a**	**30**	90
23	**6b**	**8a**	**31**	82
24	**6c**	**8a**	**32**	89
25	**6d**	**8a**	**33**	79
26	**6g**	**8a**	**34**	88
27	**6h**	**8a**	**35**	81
28	**6a**	**8b**	**36**	86
29	**6f**	**8b**	**37**	81
30	**6f**	**8c**	**38**	77
31	**7a**	**8a**	**39**	90
32	**7b**	**8a**	**40**	83

[a] Isolated yield.

15-LOX. Compounds **13** and **32** showed the highest activity against this enzyme (IC_{50} = 31 μM). However, their anti-15-LOX activity was less than that of quercetin as reference compound (IC_{50} = 18 μM). Most of active compounds had IC_{50} values in the close range of 31–45 μM, indicating the resistance of activity to the changes of the structure.

3.4. Molecular docking study

Since the most of compounds exhibited potent inhibition against cholinesterases, therefore the computational studies to determine the putative binding modes were done on both AChE and BuChE. The X-ray structures of *Torpedo californica* AChE (1ACJ) and human BuChE (4BDS) in complex with tacrine were chosen as template structures for docking studies. The latest version of Autodock was used and the entire active site was kept rigid during docking process. The putative binding mode of compound **29** (as a representative compound) in the binding sites of AChE and BuChE were depicted in Figs. 2 and 3, respectively.

As shown in Fig. 2, the hydrogen bond and the van der Waals forces are the main intramolecular interactions between compound **29** and AChE. The pyrazole fragment of the molecule was involved in hydrogen binding with Glu199, one of the catalytic triad residues, and Tyr130 as well. Moreover, a π-π stacking between pyrazole and Trp84 was detected. Similarly, Trp84 made another π-π stacking with pyridine ring that facilitates tight binding of compound **29** to the receptor. According to the docking results, the 4-fluorophenyl substituent attached to the pyran ring, positioned towards oxyanion hole and made amide-π stacking with Gly119. Finally, the cyclohexyl moiety was fitted in the hydrophobic pocket constructed by Trp84, Trp432, Phe330 and Ile439.

As depicted in Fig. 3, the hydrogen bond and the van der Waals forces are the main intramolecular interactions between compound **29** and BuChE. Two key residues of the binding site Ser198 and Trp82 are involved in binding with ligand through hydrogen bond and T-shape π-π interaction, respectively. Moreover an additional hydrogen bonding was observed between Asp70 and pyrazole ring. The phenyl ring attached to pyrazole ring made T-shape π-π interaction with Trp82 and additional H-π interaction with Ala328. The pyridine core substructure is in the T-shape π-π interaction with the Phe329 residue. In this orientation, the aliphatic cyclohexyl fragment is directed into a lipophilic pocket formed by residues Leu286, Val288 and Trp231. These features could explain why these compounds strongly inhibit BuChE.

Table 3
Inhibitory activity of synthesized compound **9**–**40** against AChE, BuChE and 15-LOX.

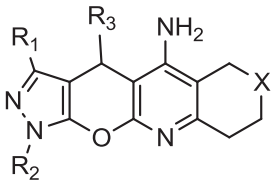

Compound	X	R_1	R_2	R_3	IC_{50} (μM) AChE	IC_{50} (μM) BuChE	SI[b]	IC_{50} (μM) 15-LOX
9	CH_2	Pr	H	Ph	–[a]	–	–	34
10	CH_2	Pr	H	4-Cl-Ph	0.200	0.010	20	45
11	CH_2	Pr	H	3-Br-Ph	0.472	0.015	31.5	39
12	CH_2	Pr	H	4-Br-Ph	–	–	–	44
13	CH_2	Pr	H	3-NO_2-Ph	0.423	0.012	35.3	31
14	CH_2	Pr	H	4-NO_2-Ph	0.744	0.029	25.7	39
15	CH_2	Pr	H	4-CN-Ph	0.954	0.037	25.8	37
16	CH_2	Pr	H	4-Me-Ph	0.120	0.013	9.2	54
17	CH_2	Pr	H	2-MeO-Ph	0.471	0.018	26.2	41
18	CH_2	Pr	H	3-MeO-Ph	–	–	–	43
19	CH_2	Pr	H	4-MeO-Ph	0.052	0.006	8.7	42
20	CH_2	Pr	H	4-MeS-Ph	0.201	0.008	25.13	35
21	CH_2	Pr	H	3,4-$(MeO)_2$-Ph	1.470	0.365	4.0	41
22	CH_2	Pr	H	3,4,5-$(MeO)_3$-Ph	0.900	0.042	21.4	45
23	CH_2	Pr	H	4-$(Me)_2$N-Ph	0.347	0.024	14.5	67
24	CH_2CH_2	Pr	H	Ph	0.650	0.043	15.1	43
25	CH_2CH_2	Pr	H	4-Cl-Ph	1.060	0.075	14.1	34
26	S	Pr	H	4-Cl-Ph	0.300	0.015	20	38
27	S	Pr	H	4-Me-Ph	1.030	0.073	14.1	51
28	CH_2	Ph	H	Ph	0.140	0.008	17.5	53
29	CH_2	Ph	H	4-F-Ph	0.034	0.007	4.9	>100
30	CH_2	Ph	H	4-Cl-Ph	0.260	0.021	12.4	>100
31	CH_2	Ph	H	4-Me-Ph	0.098	0.011	8.9	59
32	CH_2	Ph	H	4-MeO-Ph	0.081	0.007	11.6	31
33	CH_2	Ph	H	3,4,5-$(MeO)_3$-Ph	1.030	0.065	15.9	42
34	CH_2	Ph	H	Isopropyl	15.00	0.570	26.3	89
35	CH_2	Ph	Ph	Ph	>200	>200	–	>100
36	CH_2CH_2	Ph	H	Ph	0.054	0.009	6.0	53
37	CH_2CH_2	Ph	H	4-Cl-Ph	1.920	0.077	24.9	37
38	S	Ph	H	4-Cl-Ph	0.450	0.030	15.0	56
39	CH_2	2-Furyl	H	Ph	0.100	0.015	6.7	67
40	CH_2	2-Furyl	Ph	Ph	0.072	0.005	14.4	67
Tacrine					0.221	0.012	18.4	–
Quercetin					–	–	–	18

[a] Not tested.
[b] Selectivity index (IC_{50} AChE/IC_{50} BuChE).

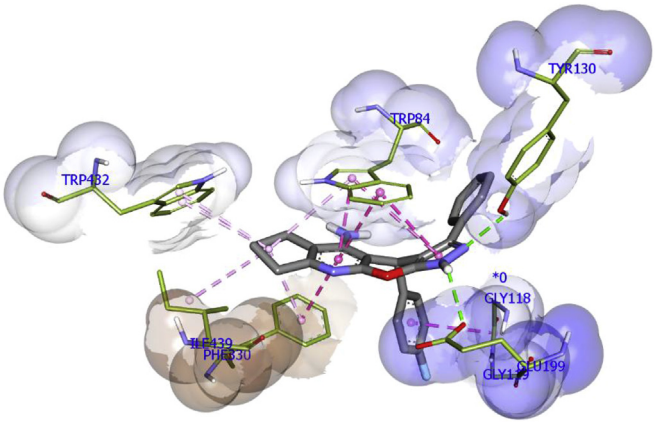

Fig. 2. The putative binding mode of compound **29** in the binding site of AChE.

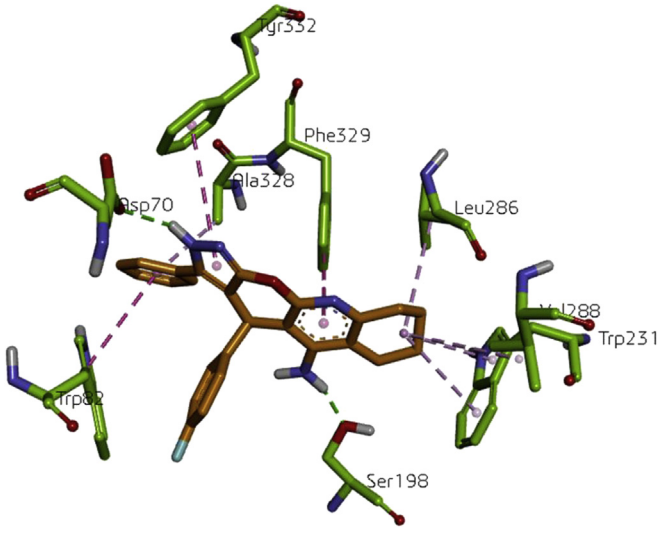

Fig. 3. The putative binding mode of compound **29** in the binding site of BuChE.

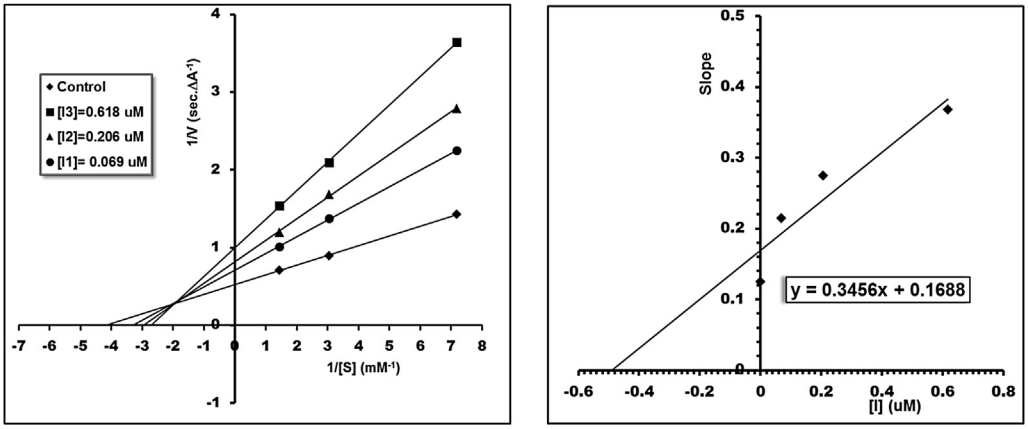

Fig. 4. *Left*: Lineweavere-Burk plot for the inhibition of AChE by compound **29** at different concentrations of substrate (ATCh), *Right*: Secondary plot for calculation of steady-state inhibition constant (K_i) of compound **29**.

Table 4
Physicochemical properties and BBB permeability of compound **9**–**40**.

Compound	Clog*P*	Log*D*	PSA (Å^2)	MW	N + O	Total H-bonds	[Clog*P*-(N + O)]	BBB Penetration	Probability
9	4.40	4.40	76.82	360.46	5	5	−0.60	+	0.963
10	5.31	5.31	76.82	394.90	5	5	0.39	+	0.946
11	5.06	5.06	76.82	439.36	5	5	0.09	+	0.940
12	5.06	5.06	76.82	439.36	5	5	0.09	+	0.940
13	4.00	4.00	122.64	404.46	8	5	−3.00	+	0.809
14	4.00	4.00	122.64	404.46	8	5	−3.00	+	0.809
15	4.23	4.23	100.61	385.47	6	5	−1.77	+	0.948
16	4.89	4.89	76.82	374.49	5	5	−0.11	+	0.957
17	4.47	4.47	86.05	390.48	6	5	−1.53	+	0.957
18	4.47	4.47	86.05	390.48	6	5	−1.53	+	0.957
19	4.47	4.47	86.05	390.48	6	5	−1.53	+	0.957
20	4.95	4.95	76.82	406.55	5	5	−0.05	+	0.937
21	4.24	4.24	95.28	420.51	7	7	−2.76	+	0.834
22	3.97	3.97	104.51	450.54	8	8	−4.03	+	0.664
23	4.89	4.89	80.06	403.53	6	6	−1.11	+	0.863
24	4.70	4.70	76.82	374.48	5	5	−0.30	+	0.964
25	5.33	5.33	76.82	408.93	5	5	0.33	+	0.949
26	4.88	4.88	76.82	412.94	5	5	−0.12	+	0.938
27	4.58	4.58	76.82	392.52	5	5	−0.42	+	0.950
28	4.70	4.70	76.82	394.48	5	5	−0.30	+	0.983
29	4.81	4.81	76.82	412.47	5	5	−0.19	+	0.982
30	5.14	5.14	76.82	428.92	5	5	0.14	+	0.976
31	5.14	5.14	76.82	408.50	5	5	0.14	+	0.975
32	4.64	4.64	86.05	424.50	6	6	−0.36	+	0.975
33	4.31	4.31	104.51	484.55	8	8	−0.69	+	0.772
34	4.48	4.48	76.82	360.46	5	5	−0.52	+	0.948
35	6.09	6.09	65.96	470.58	5	5	1.09	+	0.989
36	4.99	4.99	76.82	408.50	5	5	0.01	+	0.984
37	5.41	5.41	76.82	442.95	5	5	0.41	+	0.978
38	4.76	4.76	76.82	446.96	5	5	−0.24	+	0.9666
39	3.95	3.95	89.96	384.44	6	6	−2.05	+	0.983
40	5.31	5.31	79.10	460.54	6	6	0.31	+	0.990

Table 5
In vitro cytotoxicity of compounds **29**, **32**, and **40** on HepG2 cell line.

Compound	Viability (%)						
	1 μM	5 μM	10 μM	25 μM	50 μM	100 μM	300 μM
29	100.6 ± 0.8	100.5 ± 0.8	100.1 ± 0.6	99.7 ± 0.2	98.4 ± 0.5	89.9 ± 0.1*	73.4 ± 0.2**
32	99.1 ± 0.6	99.4 ± 0.6	99.7 ± 0.4	99.7 ± 0.6	98.2 ± 0.9	85.6 ± 1.3**	71.3 ± 0.3**
40	99.6 ± 0.1	95.8 ± 0.7	90.3 ± 1.0*	85.0 ± 0.5**	81.4 ± 1.0**	75.7 ± 1.2**	67.4 ± 0.8**
Tacrine	92.9 ± 0.6*	89.0 ± 0.8**	74.6 ± 0.7**	70.1 ± 0.5**	64.2 ± 0.6**	56.0 ± 0.5**	40.8 ± 1.0**

Data are expressed as the mean ± SEM of three independent replicates. The significant ($^{**}p \leq 0.01$, $^{*}p \leq 0.05$) values with respect to control group were obtained after one-way ANOVA analysis followed by Newman-Keuls post hoc test.

3.5. Kinetic study of AChE inhibition

The most active derivative against AChE (compound **29**) was selected for kinetic studies. For this purpose, the rate of enzyme activity was measured at four different concentrations of compound **29** as an inhibitor (0, 0.069, 0.206 and 0.618 μM) in the presence of different concentrations of substrate (acetylthiocholine iodide, ATCh). For each inhibitor concentration, the initial velocity was measured at different substrate concentrations (S) and the reciprocal of the initial velocity (1/v) was plotted versus the reciprocal of substrate concentration (1/[s]). As depicted in Fig. 4, the obtained double reciprocal (Lineweavere-Burk) plot showed a mixed-type inhibition pattern for compound **29**. The K_i value was also calculated using the secondary plot as shown in Fig. 4 (K_i = 0.49 μM). All experiments performed as same as cholinesterase inhibition test described in experimental section.

3.6. Prediction of blood-brain barrier (BBB) penetration

In order to predict the BBB permeability of the target compounds **9**–**40**, the admetSAR server (http://lmmd.ecust.edu.cn:8000/predict/) [22] was used. Furthermore, the Clark's criteria [23] was used to confirm the obtained data. The molecular descriptors were calculated by MedChem Designer (TM) version 3.1.0.30. Regarding the obtained data (Table 4), all the compounds had good BBB permeability but their extents were different relating to their structure.

3.7. Cytotoxicity on HepG2 cells

The MTT cell viability assay was applied for cytotoxicity determination. The obtained results from cytotoxicity evaluation of the most active compounds **29**, **32**, and **40** against HepG2 cell line was summarized in Table 5. In general, the cytotoxic activity of all tested compounds was lower compared to that of tacrine (Table 5). The viability percent of HepG2 cells was not significantly altered in the presence of compounds **29** and **32** (even at concentration of 50 μM) compared to that of control while tacrine decreased the viability into 64.2% ($p \leq 0.01$) at the same concentration. In the case of compound **40** (50 μM) the viability percent was found to be 81.4% which was higher than that of tacrine. In general, the selected compounds showed less toxicity on HepG2 cells compared to Tacrine.

4. Conclusion

We have synthesized a series of tacrine-based pyrazolo [4′,3′:5,6]pyrano [2,3-*b*]quinolines and related compounds targeting AChE, BuChE and 15-LOX enzymes in the field of Alzheimer's disease therapy. The SAR of designed compounds was studied by introducing poly-functionality on the core structure particularly on the pyrazolopyran scaffold. Most of compounds showed potent activity against cholinesterases and mild potency toward 15-LOX enzyme. Representatively, compounds **29**, **32** and **40** displayed inhibition at nano-molar level against AChE and BuChE (IC_{50}s = 0.005–0.08 μM), being more potent than reference drug tacrine. Moreover, compound **32** with IC_{50} value of 31 μM was the most potent compound against 15-LOX. The SAR studies revealed that the tetracyclic core structure has adequate tolerability for multi-functional substitutions in order to modulate their action on multi-targets useful in the AD therapy.

5. Experimental

All starting materials were commercial products, and were used without further purification with the exception of liquid aldehydes which were purified by using standard procedures prior to use. Nuclear magnetic resonance spectra were obtained on a FT-NMR Bruker Ultra Shield™ (500 MHz for ^{1}H and 125 MHz for ^{13}C) or Bruker DRX-400 AVANCE (400 MHz for ^{1}H and 100 MHz for ^{13}C) instruments in DMSO-d_6 using TMS as a standard. Mass spectra were obtained on an Agilent Technology (HP), 5973 Network Mass Selective Detector and Agilent Technology (HP), 5973 Network Mass Selective Detector at ionization potential of 70 eV. FT-IR spectra were recorded using KBr disks on a Bruker Vector-22 infrared spectrometer and absorptions were reported as wave numbers (cm^{-1}). Elemental analyses were carried out by a CHN-Rapid Heraeus elemental analyzer. The results of elemental analyses (C, H, N) were within ±0.4% of the calculated values.

5.1. General procedure for the preparation of intermediates *5*–*7*

In a 100 mL round bottom flask, a mixture of hydrazine hydrate/phenyl hydrazine (**1**, 12 mmol), β-ketoester (**2**, 10 mmol), malononitrile (**3**, 10 mmol), (*S*)-proline (10% mol) and water (20 mL) were taken and the mixture was irradiated in the ultrasonic bath for 2 min. Afterward, appropriate aldehyde (**4**, 10 mmol) was added to the mixture and the mixture was irradiated for 10–30 min. Progress of the reaction was monitored by TLC. After completion of the reaction, the precipitated solid was filtered and recrystallized from ethanol.

5.2. General procedure for the preparation of final compounds *9*–*40*

Aluminum chloride (1.5 equiv.) was suspended in dry 1,2-dichloroethane (10 mL) at room temperature under argon atmosphere. After stirring the suspension for a few minutes, the corresponding pyrano[2,3-*c*]pyrazole (**5**–**7**, 1 equiv.) and ketone **8** (1.5 equiv.) were added to the mixture and the reaction mixture was heated under reflux for 24 h. Progress of the reaction was monitored by TLC. After completion of the reaction, an aqueous solution of sodium hydroxide (10%) was added dropwise to the mixture until the aqueous solution became basic. After stirring for 30 min, the precipitate was filtered and washed with water. The structure of new products was determined by their physical and spectroscopic specifications and their purity was confirmed by elemental analyses.

5.2.1. 4-Phenyl-3-propyl-2,4,6,7,8,9-hexahydropyrazolo[4′,3′:5,6]pyrano[2,3-b]quinolin-5-amine ***(9)***

Yield 87%; Cream white solid; mp > 250 °C; IR (KBr, cm^{-1}) ν_{max}: 3474 and 3361 (NH_2), 1580 (C=N); ^{1}H NMR (DMSO-d_6, 500 MHz) δ: 11.86 (brs, 1H, NH), 7.25–7.22 (m, 4H, phenyl), 7.12–7.10 (m, 1H, phenyl), 5.38 (brs, 2H, NH_2), 5.19 (s, 1H, H_4), 2.57 (m, 2H, CH_2), 2.33–2.18 (m, 4H, $2CH_2$), 1.70–1.69 (m, 4H, $2CH_2$), 1.39–1.25 (m, 2H, CH_2), 0.69 (brs, 3H, CH_3); ^{13}C NMR (DMSO-d_6, 125 MHz) δ: 156.3, 155.5, 152.4, 152.0, 145.5, 139.1, 128.3, 127.4, 126.2, 111.9, 99.5, 98.7, 34.2, 32.0, 26.3, 22.9, 22.3, 22.1, 21.2, 13.3; Anal. Calcd for $C_{22}H_{24}N_4O$: C, 73.31; H, 6.71; N, 15.54. Found: C, 73.04; H, 6.42; N, 15.62.

5.2.2. 4-(4-Chlorophenyl)-3-propyl-2,4,6,7,8,9-hexahydropyrazolo[4′,3′:5,6]pyrano[2,3-b]quinolin-5-amine ***(10)***

Yield 93%; White solid; mp > 250 °C; IR (KBr, cm^{-1}) ν_{max}: 3500 and 3403 (NH_2), 1578 (C=N); ^{1}H NMR (DMSO-d_6, 500 MHz) δ: 11.88 (brs, 1H, NH), 7.25 (brs, 4H, phenyl), 5.43 (brs, 2H, NH_2), 5.22 (s, 1H, H_4), 2.55–2.53 (m, 2H, CH_2), 2.31–2.12 (m, 4H, $2CH_2$), 1.67–1.65 (m, 4H, $2CH_2$), 1.42–1.26 (m, 2H, CH_2), 0.69 (t, J = 7.5 Hz, 3H, CH_3); ^{13}C NMR (DMSO-d_6, 125 MHz) δ: 157.2, 156.3, 153.3, 152.9, 145.4, 140.0, 131.5, 130.1, 129.1, 112.9, 100.0, 99.2, 34.3, 32.9, 27.2, 23.8, 23.2, 23.0,

22.1, 14.2; MS (*m/z*, %): 394 (M^+, 32), 396 (M+2,11), 350 (7), 282 (100), 253 (11); Anal. Calcd for $C_{22}H_{23}ClN_4O$: C, 66.91; H, 5.87; N, 14.19. Found: C, 66.73; H, 5.99; N, 14.30.

5.2.3. 4-(3-Bromophenyl)-3-propyl-2,4,6,7,8,9-hexahydropyrazolo [4′,3′:5,6]pyrano[2,3-b]quinolin-5-amine ***(11)***

Yield 87%; White solid; mp > 250 °C; IR (KBr, cm^{-1}) ν_{max}: 3412 and 3353 (NH_2), 1580 (C═N); ^1H NMR (DMSO-d_6, 500 MHz) δ: 11.94 (brs, 1H, NH), 7.52 (s, 1H, phenyl), 7.33–7.31 (m, 1H, phenyl), 7.19–7.18 (m, 2H, phenyl), 5.51 (brs, 2H, NH_2), 5.25 (s, 1H, H_4), 2.58 (brs, 2H, CH_2), 2.38–2.16 (m, 4H, $2CH_2$), 1.71–1.69 (m, 4H, $2CH_2$), 1.46–1.21 (m, 2H, CH_2), 0.71 (t, J = 7.5 Hz, 3H, CH_3); ^{13}C NMR (DMSO-d_6, 125 MHz) δ: 156.3, 155.4, 152.5, 152.0, 148.3, 139.2, 130.6, 130.0, 129.1, 126.5, 121.4, 112.1, 99.0, 98.1, 33.6, 32.0, 26.3, 22.9, 22.3, 22.1, 21.3, 13.4; Anal. Calcd for $C_{22}H_{23}BrN_4O$: C, 60.14; H, 5.28; N, 12.75. Found: C, 60.43; H, 5.07; N, 12.92.

5.2.4. 4-(4-Bromophenyl)-3-propyl-2,4,6,7,8,9-hexahydropyrazolo [4′,3′:5,6]pyrano[2,3-b]quinolin-5-amine ***(12)***

Yield 92%; Cream white solid; mp > 250 °C; IR (KBr, cm^{-1}) ν_{max}: 3501 and 3403 (NH_2), 1579 (C═N); ^1H NMR (DMSO-d_6, 500 MHz) δ: 11.91 (brs, 1H, NH), 7.41 (d, J = 8.0 Hz, 2H, phenyl), 7.22 (d, J = 8.0 Hz, 2H, phenyl), 5.45 (brs, 2H, NH_2), 5.24 (s, 1H, H_4), 2.58–2.56 (m, 2H, CH_2), 2.34–2.16 (m, 4H, $2CH_2$), 1.70–1.69 (m, 4H, $2CH_2$), 1.48–1.29 (m, 2H, CH_2), 0.73 (t, J = 7.5 Hz, 3H, CH_3); ^{13}C NMR (DMSO-d_6, 125 MHz) δ: 156.3, 155.4, 152.4, 152.0, 144.9, 139.1, 131.1, 129.6, 119.1, 112.0, 99.0, 98.3, 33.4, 32.0, 26.3, 22.9, 22.3, 22.1, 21.2, 13.3; Anal. Calcd for $C_{22}H_{23}BrN_4O$: C, 60.14; H, 5.28; N, 12.75. Found: C, 60.02; H, 5.41; N, 12.98.

5.2.5. 4-(3-Nitrophenyl)-3-propyl-2,4,6,7,8,9-hexahydropyrazolo [4′,3′:5,6]pyrano[2,3-b]quinolin-5-amine ***(13)***

Yield 90%; White solid; mp > 250 °C; IR (KBr, cm^{-1}) ν_{max}: 3376 and 3233 (NH_2), 1578 (C═N); ^1H NMR (DMSO-d_6, 500 MHz) δ: 12.00 (brs, 1H, NH), 8.30 (s, 1H, phenyl), 8.01 (d, J = 7.5 Hz, 1H, phenyl), 7.60 (d, J = 7.0 Hz, 1H, phenyl), 7.53 (d, J = 7.0 Hz, 1H, phenyl), 5.63 (brs, 2H, NH_2), 5.48 (s, 1H, H_4), 2.58–2.56 (m, 2H, CH_2), 2.33–2.14 (m, 4H, $2CH_2$), 1.71–1.69 (m, 4H, $2CH_2$), 1.45–1.25 (m, 2H, CH_2), 0.69 (t, J = 7.0 Hz, 3H, CH_3); ^{13}C NMR (DMSO-d_6, 125 MHz) δ: 156.4, 155.4, 152.7, 152.1, 147.8, 147.4, 139.3, 134.1, 130.0, 121.8, 121.4, 112.2, 98.7, 97.9, 33.4, 32.0, 26.3, 22.9, 22.2, 22.0, 21.2, 13.3; Anal. Calcd for $C_{22}H_{23}N_5O_3$: C, 65.17; H, 5.72; N, 17.27. Found: C, 65.05; H, 5.56; N, 17.41.

5.2.6. 4-(4-Nitrophenyl)-3-propyl-2,4,6,7,8,9-hexahydropyrazolo [4′,3′:5,6]pyrano[2,3-b]quinolin-5-amine ***(14)***

Yield 93%; Cream white solid; mp > 250 °C; IR (KBr, cm^{-1}) ν_{max}: 3503 and 3407 (NH_2), 1580 (C═N); ^1H NMR (DMSO-d_6, 500 MHz) δ: 12.00 (brs, 1H, NH), 8.14 (d, J = 8.5 Hz, 2H, phenyl), 7.55 (d, J = 8.5 Hz, 2H, phenyl), 5.58 (brs, 2H, NH_2), 5.48 (s, 1H, H_4), 2.59–2.57 (m, 2H, CH_2), 2.35–2.14 (m, 4H, $2CH_2$), 1.71–1.68 (m, 4H, $2CH_2$), 1.50–1.30 (m, 2H, CH_2), 0.73 (t, J = 7.0 Hz, 3H, CH_3); ^{13}C NMR (DMSO-d_6, 125 MHz) δ: 155.4, 153.1, 152.8, 152.1, 145.9, 139.4, 128.6, 123.6, 112.2, 98.4, 97.8, 33.7, 32.0, 26.3, 22.9, 22.3, 22.1, 21.2, 13.3; Anal. Calcd for $C_{22}H_{23}N_5O_3$: C, 65.17; H, 5.72; N, 17.27. Found: C, 65.29; H, 5.56; N, 17.46.

5.2.7. 4-(5-Amino-3-propyl-2,4,6,7,8,9-hexahydropyrazolo [4′,3′:5,6]pyrano[2,3-b]quinolin-4-yl)benzonitrile ***(15)***

Yield 84%; White solid; mp > 250 °C; IR (KBr, cm^{-1}) ν_{max}: 3505 and 3408 (NH_2), 1581 (C═N); ^1H NMR (DMSO-d_6, 500 MHz) δ: 11.97 (brs, 1H, NH), 7.71 (d, J = 8.0 Hz, 2H, phenyl), 7.46 (d, J = 8.0 Hz, 2H, phenyl), 5.54 (brs, 2H, NH_2), 5.38 (s, 1H, H_4), 2.58–2.56 (m, 2H, CH_2), 2.33–2.14 (m, 4H, $2CH_2$), 1.71–1.69 (m, 4H, $2CH_2$), 1.47–1.29 (m, 2H, CH_2), 0.70 (t, J = 7.5 Hz, 3H, CH_3); ^{13}C NMR (DMSO-d_6, 125 MHz) δ: 156.4, 155.5, 152.7, 152.1, 151.1, 139.3, 132.3, 128.4, 118.8, 112.1, 109.0, 98.6, 98.0, 34.0, 32.0, 26.3, 22.9, 22.3, 22.1, 21.2, 13.3; Anal. Calcd for $C_{23}H_{23}N_5O$: C, 71.67; H, 6.01; N, 18.17. Found: C, 71.83; H, 5.81; N, 18.35.

5.2.8. 3-Propyl-4-(p-tolyl)-2,4,6,7,8,9-hexahydropyrazolo[4′,3′:5,6] pyrano[2,3-b]quinolin-5-amine ***(16)***

Yield 89%; White solid; mp > 250 °C; IR (KBr, cm^{-1}) ν_{max}: 3496 and 3399 (NH_2), 1578 (C═N); ^1H NMR (DMSO-d_6, 400 MHz) δ: 11.92 (brs, 1H, NH), 7.13 (d, J = 7.6 Hz, 2H, phenyl), 7.02 (d, J = 7.6 Hz, 2H, phenyl), 5.35 (brs, 2H, NH_2), 5.13 (s, 1H, H_4), 2.57–2.53 (m, 2H, CH_2), 2.33–2.28 (m, 4H, CH_2), 2.19 (s, 3H, CH_3-phenyl), 1.70–1.68 (m, 4H, $2CH_2$), 1.46–1.23 (m, 2H, CH_2), 0.72 (t, J = 7.2 Hz, 3H, CH_3); ^{13}C NMR (DMSO-d_6, 100 MHz) δ: 156.7, 155.9, 152.6, 152.4, 142.9, 139.6, 135.6, 129.3, 127.8, 112.4, 100.0, 99.3, 34.3, 32.4, 26.8, 23.3, 22.8, 22.6, 21.7, 21.0, 13.9; MS (*m/z*, %): 374 (M^+, 48), 331 (13), 283 (100), 254 (20); Anal. Calcd for $C_{23}H_{26}N_4O$: C, 73.77; H, 7.00; N, 14.96. Found: C, 73.82; H, 6.92; N, 14.82%.

5.2.9. 4-(2-Methoxyphenyl)-3-propyl-2,4,6,7,8,9-hexahydropyrazolo[4′,3′:5,6]pyrano[2,3-b]quinolin-5-amine ***(17)***

Yield 82%; Cream solid; mp > 250 °C; IR (KBr, cm^{-1}) ν_{max}: 3479 and 3386 (NH_2), 1581 (C═N); ^1H NMR (DMSO-d_6, 500 MHz) δ: 11.85 (brs, 1H, NH), 7.14 (d, J = 7.0 Hz, 1H, phenyl), 7.03 (d, J = 7.5 Hz, 1H, phenyl), 6.90–6.70 (m, 2H, phenyl), 5.33 (s, 1H, H_4), 5.20 (brs, 2H, NH_2), 3.91 (s, 3H, OCH_3), 2.57–2.53 (m, 2H, CH_2), 2.25–2.20 (m, 4H, $2CH_2$), 1.70–1.68 (m, 4H, $2CH_2$), 1.28–1.13 (m, 2H, CH_2), 0.62 (brs, 3H, CH_3); ^{13}C NMR (DMSO-d_6, 125 MHz) δ: 156.7, 155.5, 154.8, 152.0, 151.7, 139.0, 132.8, 129.6, 127.6, 121.4, 111.7, 110.8, 99.2, 98.7, 55.8, 31.9, 26.8, 26.3, 22.8, 22.3, 22.1, 21.1, 13.3; Anal. Calcd for $C_{23}H_{26}N_4O_2$: C, 70.75; H, 6.71; N, 14.35. Found: C, 70.96; H, 6.83; N, 14.21.

5.2.10. 4-(3-Methoxyphenyl)-3-propyl-2,4,6,7,8,9-hexahydropyrazolo[4′,3′:5,6]pyrano[2,3-b]quinolin-5-amine ***(18)***

Yield 84%; Cream white solid; mp > 250 °C; IR (KBr, cm^{-1}) ν_{max}: 3494 and 3363 (NH_2), 1585 (C═N); ^1H NMR (DMSO-d_6, 500 MHz) δ: 11.87 (brs, 1H, NH), 7.13 (d, J = 7.5 Hz, 1H, phenyl), 6.93 (s, 1H, phenyl), 6.73 (d, J = 7.5, Hz, 1H, phenyl), 6.70 (d, J = 7.5 Hz, 1H, phenyl), 5.40 (brs, 2H, NH_2), 5.16 (s, 1H, H_4), 3.68 (s, 3H, OCH_3), 2.58–2.56 (m, 2H, CH_2), 2.36–2.17 (m, 4H, $2CH_2$), 1.72–1.69 (m, 4H, $2CH_2$), 1.44–1.24 (m, 2H, CH_2), 0.72 (t, J = 7.0 Hz, 3H, CH_3); ^{13}C NMR (DMSO-d_6, 125 MHz) δ: 159.0, 156.3, 155.5, 152.3, 152.1, 147.0, 139.2, 129.5, 119.7, 113.9, 111.9, 110.8, 99.3, 98.5, 54.9, 34.2, 32.0, 26.4, 22.9, 22.3, 22.1, 21.3, 13.4; Anal. Calcd for $C_{23}H_{26}N_4O_2$: C, 70.75; H, 6.71; N, 14.35. Found: C, 70.57; H, 6.43; N, 14.11.

5.2.11. 4-(4-Methoxyphenyl)-3-propyl-2,4,6,7,8,9-hexahydropyrazolo[4′,3′:5,6]pyrano[2,3-b]quinolin-5-amine ***(19)***

Yield 88%; White solid; mp > 250 °C; IR (KBr, cm^{-1}) ν_{max}: 3496 and 3400 (NH_2), 1578 (C═N); ^1H NMR (DMSO-d_6, 500 MHz) δ: 11.84 (brs, 1H, NH), 7.16 (d, J = 8.0 Hz, 2H, phenyl), 6.78 (d, J = 8.0 Hz, 2H, phenyl), 5.36 (brs, 2H, NH_2), 5.12 (s, 1H, H_4), 3.67 (s, 3H, OCH_3), 2.57–2.53 (m, 2H, CH_2), 2.34–2.15 (m, 4H, $2CH_2$), 1.70–1.68 (m, 4H, $2CH_2$), 1.45–1.23 (m, 2H, CH_2), 0.72 (t, J = 7.5 Hz, 3H, CH_3); ^{13}C NMR (DMSO-d_6, 125 MHz) δ: 157.5, 156.3, 155.4, 152.1, 152.0, 139.0, 137.5, 128.4, 113.6, 111.9, 99.7, 98.9, 54.9, 33.4, 32.0, 26.3, 22.9, 22.4, 22.1, 21.3, 13.4; Anal. Calcd for $C_{23}H_{26}N_4O_2$: C, 70.75; H, 6.71; N, 14.35. Found: C, 70.96; H, 6.79; N, 14.11.

5.2.12. 4-(4-(Methylthio)phenyl)-3-propyl-2,4,6,7,8,9-hexahydropyrazolo[4′,3′:5,6]pyrano[2,3-b]quinolin-5-amine ***(20)***

Yield 85%; Light yellow solid; mp > 250 °C; IR (KBr, cm^{-1}) ν_{max}: 3496 and 3402 (NH_2), 1576 (C═N); ^1H NMR (DMSO-d_6, 500 MHz) δ: 11.87 (brs, 1H, NH), 7.20 (d, J = 8.0 Hz, 2H, phenyl), 7.11 (d, J = 8.0 Hz,

2H, phenyl), 5.39 (brs, 2H, NH_2), 5.17 (s, 1H, H_4), 2.54–2.52 (m, 2H, CH_2), 2.39 (s, 3H, SCH_3), 2.36–2.16 (m, 4H, $2CH_2$), 1.71–1.69 (m, 4H, $2CH_2$), 1.48–1.29 (m, 2H, CH_2), 0.73 (t, $J = 7.5$ Hz, 3H, CH_3); ^{13}C NMR (DMSO-d_6, 125 MHz) δ: 156.3, 155.4, 152.2, 152.0, 142.2, 139.1, 138.9, 135.5, 128.0, 126.0, 111.9, 99.3, 98.6, 33.6, 32.0, 26.3, 22.9, 22.3, 22.1, 21.2, 14.8, 13.4; Anal. Calcd for $C_{23}H_{26}N_4OS$: C, 67.95; H, 6.45; N, 13.78. Found: C, 67.81; H, 6.27; N, 13.99.

5.2.13. 4-(3,4-Dimethoxyphenyl)-3-propyl-2,4,6,7,8,9-hexahydropyrazolo[4′,3′:5,6]pyrano[2,3-b]quinolin-5-amine ***(21)***

Yield 82%; Cream solid; mp > 250 °C; IR (KBr, cm^{-1}) ν_{max}: 3503 and 3407 (NH_2), 1577 (C=N); ^1H NMR (DMSO-d_6, 500 MHz) δ: 11.85 (brs, 1H, NH), 7.06 (d, $J = 1.0$ Hz, 1H, phenyl), 6.80 (d, $J = 8.5$ Hz, 1H, phenyl), 6.62 (dd, $J = 8.5$ and 1.0 Hz, 1H, phenyl), 5.36 (brs, 2H, NH_2), 5.10 (s, 1H, H_4), 3.69 (s, 3H, OCH_3), 3.66 (s, 3H, OCH_3), 2.57 (brs, 2H, CH_2), 2.40–2.17 (m, 4H, $2CH_2$), 1.71–1.69 (m, 4H, $2CH_2$), 1.46–1.25 (m, 2H, CH_2), 0.74 (t, $J = 7.0$ Hz, 3H, CH_3); ^{13}C NMR (DMSO-d_6, 125 MHz) δ: 155.5, 152.1, 152.1, 148.2, 147.1, 139.1, 138.9, 138.0, 119.4, 112.1, 111.8, 99.6, 98.7, 55.5, 55.4, 33.9, 32.0, 26.5, 22.9, 22.4, 22.1, 21.3, 13.5; Anal. Calcd for $C_{24}H_{28}N_4O_3$: C, 68.55; H, 6.71; N, 13.32. Found: C, 68.76; H, 6.43; N, 13.10.

5.2.14. 3-Propyl-4-(3,4,5-trimethoxyphenyl)-2,4,6,7,8,9-hexahydropyrazolo[4′,3′:5,6]pyrano[2,3-b]quinolin-5-amine ***(22)***

Yield 87%; White solid; mp > 250 °C; IR (KBr, cm^{-1}) ν_{max}: 3506 and 3412 (NH_2), 1591 (C=N); ^1H NMR (DMSO-d_6, 500 MHz) δ: 11.99 (brs, 1H, NH), 6.62 (s, 2H, phenyl), 5.84 (brs, 2H, NH_2), 5.16 (s, 1H, H_4), 3.66 (s, 6H, $2OCH_3$), 3.58 (s, 3H, OCH_3), 2.62–2.58 (m, 2H, CH_2), 2.37–2.21 (m, 4H, $2CH_2$), 1.73–1.70 (m, 4H, $2CH_2$), 1.43–1.26 (m, 2H, CH_2), 0.72 (t, $J = 6.5$ Hz, 3H, CH_3); ^{13}C NMR (DMSO-d_6, 125 MHz) δ: 156.1, 155.6, 152.7, 151.1, 140.5, 139.5, 136.0, 111.9, 105.0, 98.9, 98.2, 59.9, 55.9, 34.4, 31.1, 26.4, 22.7, 21.9, 21.8, 21.3, 13.5; MS (*m*/*z*, %): 450 (M^+, 22), 370 (33), 283 (100); Anal. Calcd for $C_{25}H_{30}N_4O_4$: C, 66.65; H, 6.71; N, 12.44. Found: 66.58; H, 6.63; N, 12.31.

5.2.15. 4-(4-(Dimethylamino)phenyl)-3-propyl-2,4,6,7,8,9-hexahydropyrazolo[4′,3′:5,6]pyrano[2,3-b]quinolin-5-amine ***(23)***

Yield 81%; Yellow solid; mp > 250 °C; IR (KBr, cm^{-1}) ν_{max}: 3481 and 3388 (NH_2), 1576 (C=N); ^1H NMR (DMSO-d_6, 500 MHz) δ: 11.80 (brs, 1H, NH), 7.05 (d, $J = 8.0$ Hz, 2H, phenyl), 6.58 (d, $J = 8.0$ Hz, 2H, phenyl), 5.27 (brs, 2H, NH_2), 5.00 (s, 1H, H_4), 2.80 (s, 6H, $N(CH_3)_2$), 2.57–2.55 (m, 2H, CH_2), 2.31–2.17 (m, 4H, $2CH_2$), 1.71–1.69 (m, 4H, $2CH_2$), 1.45–1.28 (m, 2H, CH_2), 0.74 (t, $J = 7.0$ Hz, 3H, CH_3); ^{13}C NMR (DMSO-d_6, 125 MHz) δ: 156.3, 155.4, 152.0, 151.9, 148.9, 139.0, 133.0, 127.9, 112.4, 111.8, 99.8, 99.1, 40.2, 33.5, 32.0, 26.4, 22.9, 22.4, 22.1, 21.3, 13.5; Anal. Calcd for $C_{24}H_{29}N_5O$: C, 71.44; H, 7.24; N, 17.36. Found: C, 71.25; H, 7.41; N, 17.03.

5.2.16. 4-Phenyl-3-propyl-4,6,7,8,9,10-hexahydro-2H-cyclohepta[b]pyrazolo[4′,3′:5,6]pyrano[3,2-e]pyridin-5-amine ***(24)***

Yield 85%; Cream white solid; mp > 250 °C; IR (KBr, cm^{-1}) ν_{max}: 3463 and 3327 (NH_2), 1585 (C=N); ^1H NMR (DMSO-d_6, 500 MHz) δ: 11.94 (brs, 1H, NH), 7.26–7.20 (m, 4H, phenyl), 7.13–7.10 (m, 1H, phenyl), 5.42 (brs, 2H, NH_2), 5.17 (s, 1H, H_4), 2.79–2.67 (m, 2H, CH_2), 2.60–2.41 (m, 2H, CH_2), 2.33–2.29 (m, 2H, CH_2), 1.78–1.66 (m, 2H, CH_2), 1.50–1.45 (m, 2H, CH_2), 1.40–1.32 (m, 2H, CH_2), 1.27–1.23 (m, 2H, CH_2), 0.69 (t, $J = 6.0$ Hz, 3H, CH_3); ^{13}C NMR (DMSO-d_6, 125 MHz) δ: 159.2, 156.3, 155.2, 151.4, 145.5, 139.2, 128.3, 126.2, 117.1, 99.5, 99.4, 37.9, 34.6, 31.7, 27.0, 26.3, 26.0, 24.7, 21.2, 13.4; Anal. Calcd for $C_{23}H_{26}N_4O$: C, 73.77; H, 7.00; N, 14.96. Found: C, 73.85; H, 6.85; N, 14.81.

5.2.17. 4-(4-Chlorophenyl)-3-propyl-4,6,7,8,9,10-hexahydro-2H-cyclohepta[b]pyrazolo[4′,3′:5,6]pyrano[3,2-e]pyridin-5-amine ***(25)***

Yield 86%; White solid; mp > 250 °C; IR (KBr, cm^{-1}) ν_{max}: 3421 and 3327 (NH_2), 1572 (C=N); ^1H NMR (DMSO-d_6, 500 MHz) δ: 11.89 (brs, 1H, NH), 7.29 (d, $J = 9.0$ Hz, 2H, phenyl), 7.26 (d, $J = 9.0$ Hz, 2H, phenyl), 5.49 (brs, 2H, NH_2), 5.22 (s, 1H, H_4), 2.78–2.68 (m, 2H, CH_2), 2.61–2.41 (m, 2H, CH_2), 2.34–2.28 (m, 2H, CH_2), 1.78–1.40 (m, 6H, $3CH_2$), 1.36–1.29 (m, 2H, CH_2), 0.73 (t, $J = 7.5$ Hz, 3H, CH_3); ^{13}C NMR (DMSO-d_6, 125 MHz) δ: 159.3, 156.2, 155.1, 151.3, 144.5, 139.1, 130.7, 129.2, 128.2, 117.2, 99.1, 37.9, 33.7, 31.7, 26.9, 26.3, 26.0, 24.7, 21.2, 13.3; Anal. Calcd for $C_{23}H_{25}ClN_4O$: C, 67.55; H, 6.16; N, 13.70. Found: C, 67.79; H, 6.22; N, 13.63.

5.2.18. 4-(4-Chlorophenyl)-3-propyl-4,6,8,9-tetrahydro-2H-pyrazolo[4′,3′:5,6]pyrano[2,3-b]thiopyrano[3,4-e]pyridin-5-amine ***(26)***

Yield 89%; Cream white solid; mp > 250 °C; IR (KBr, cm^{-1}) ν_{max}: 3500 and 3406 (NH_2), 1578 (C=N); ^1H NMR (DMSO-d_6, 500 MHz) δ: 11.93 (brs, 1H, NH), 7.26 (brs, 4H, phenyl), 5.65 (brs, 2H, NH_2), 5.26 (s, 1H, H_4), 3.86–3.79 (m, 2H, CH_2), 3.48–3.22 (m, 4H, $2CH_2$), 2.47 (s, 2H, CH_2), 2.33–2.28 (m, 2H, CH_2), 0.69 (t, $J = 7.5$ Hz, 3H, CH_3); ^{13}C NMR (DMSO-d_6, 125 MHz) δ: 157.0, 156.5, 152.8, 152.3, 145.1, 140.1, 131.6, 130.1, 129.1, 120.7, 111.3, 99.9, 45.9, 34.5, 34.3, 25.6, 24.4, 22.1, 14.2; MS (*m*/*z*, %): 412 (M^+, 12), 414 (6, M^++2), 301 (100), 255 (20); Anal. Calcd for $C_{21}H_{21}ClN_4OS$: C, 61.08; H, 5.13; N, 13.57. Found: C, 60.81; H, 5.39; N, 13.62.

5.2.19. 3-Propyl-4-(p-tolyl)-4,6,8,9-tetrahydro-2H-pyrazolo[4′,3′:5,6]pyrano[2,3-b]thiopyrano[3,4-e]pyridin-5-amine ***(27)***

Yield 86%; Cream white solid; mp > 250 °C; IR (KBr, cm^{-1}) ν_{max}: 3494 and 3400 (NH_2), 1576 (C=N); ^1H NMR (DMSO-d_6, 500 MHz) δ: 11.86 (brs, 1H, NH), 7.11 (d, $J = 7.6$ Hz, 2H, phenyl), 7.00 (d, $J = 7.6$ Hz, 2H, phenyl), 5.54 (brs, 2H, NH_2), 5.14 (s, 1H, H_4), 3.46–3.40 (m, 2H, CH_2), 2.84–2.80 (m, 4H, $2CH_2$), 2.29 (s, 2H, CH_2), 2.16 (s, 3H, CH_3), 1.42–1.24 (m, 2H, CH_2), 0.69 (t, $J = 7.2$ Hz, 3H, CH_3); ^{13}C NMR (DMSO-d_6, 125 MHz) δ: 157.1, 156.6, 152.5, 152.2, 143.1, 140.0, 136.1, 129.7, 128.2, 111.2, 100.3, 34.7, 34.5, 27.2, 25.6, 24.3, 22.1, 21.4, 14.3; MS (*m*/*z*, %): 392 (M^+, 70), 300 (100), 278 (85), 249 (43); Anal. Calcd for $C_{22}H_{24}N_4OS$: C, 67.32; H, 6.16; N, 14.27. Found: C, 67.40; H, 6.02; N, 14.46.

5.2.20. 3,4-Diphenyl-2,4,6,7,8,9-hexahydropyrazolo[4′,3′:5,6]pyrano[2,3-b]quinolin-5-amine ***(28)***

Yield 92%; White solid; mp > 250 °C; IR (KBr, cm^{-1}) ν_{max}: 3352 and 3181 (NH_2), 1640 (C=N); ^1H NMR (DMSO-d_6, 500 MHz) δ: 13.18 (brs, 1H, NH), 7.77–7.08 (m, 12H, 2phenyl and NH_2), 6.01 (s, 1H, H_4), 2.77–2.75 (m, 2H, CH_2), 2.41–2.20 (m, 2H, CH_2), 1.78–1.70 (m, 4H, $2CH_2$); ^{13}C NMR (DMSO-d_6, 125 MHz) δ: 157.0, 155.0, 150.8, 145.4, 142.7, 138.2, 128.8, 128.4, 128.3, 127.6, 126.9, 126.4, 112.8, 99.6, 99.2, 32.9, 26.5, 22.2, 20.7, 20.4; Anal. Calcd for $C_{25}H_{22}N_4O$: C, 76.12; H, 5.62; N, 14.20. Found: C, 76.03; H, 5.97; N, 14.19.

5.2.21. 4-(4-Fluorophenyl)-3-phenyl-2,4,6,7,8,9-hexahydropyrazolo[4′,3′:5,6]pyrano[2,3-b]quinolin-5-amine ***(29)***

Yield 94%; White solid; mp > 250 °C; IR (KBr, cm^{-1}) ν_{max}: 3341 and 3213 (NH_2), 1648 (C=N); ^1H NMR (DMSO-d_6, 500 MHz) δ: 12.90 (brs, 1H, NH), 7.74–6.96 (m, 9H, phenyl), 6.62 (brs, 2H, NH_2), 5.85 (s, 1H, H_4), 2.67–2.65 (m, 2H, CH_2), 2.39–2.18 (m, 2H, CH_2), 1.73–1.71 (m, 4H, $2CH_2$); ^{13}C NMR (DMSO-d_6, 125 MHz) δ: 160.7 (d, $J = 245.0$ Hz), 156.6, 153.1, 149.4, 140.0, 137.7, 129.4 (d, $J = 8.0$ Hz), 128.8, 128.5, 126.3, 114.8 (d, $J = 21.0$ Hz), 112.5, 99.8, 99.3, 60.1, 32.7, 29.5, 22.6, 21.5; Anal. Calcd for $C_{25}H_{21}FN_4O$: C, 72.80; H, 5.13; N, 13.58. Found: C, 72.67; H, 5.23; N, 13.39.

*5.2.22. 4-(4-Chlorophenyl)-3-phenyl-2,4,6,7,8,9-hexahydropyrazolo[4′,3′:5,6]pyrano[2,3-b]quinolin-5-amine (**30**)*

Yield 90%; White solid; mp > 250 °C; IR (KBr, cm^{-1}) ν_{max}: 3341 and 3219 (NH_2), 1648 (C=N); ^1H NMR (DMSO-d_6, 500 MHz) δ:

12.88 (brs, 1H, NH), 7.72–7.19 (m, 9H, phenyl), 6.48 (brs, 2H, NH_2), 5.83 (s, 1H, H_4), 2.64–2.62 (m, 2H, CH_2), 2.39–2.18 (m, 2H, CH_2), 1.73–1.70 (m, 4H, $2CH_2$); ^{13}C NMR (DMSO-d_6, 125 MHz) δ: 156.8, 153.8, 142.9, 137.7, 131.0, 129.3, 128.8, 128.5, 128.0, 126.2, 112.5, 99.4, 99.0, 32.9, 29.5, 22.7, 21.6; Anal. Calcd for $C_{25}H_{21}ClN_4O$: C, 70.01; H, 4.93; N, 13.06. Found: C, 69.82; H, 4.74; N, 13.37.

5.2.23. 3-Phenyl-4-(p-tolyl)-2,4,6,7,8,9-hexahydropyrazolo [4′,3′:5,6]pyrano[2,3-b]quinolin-5-amine ***(31)***

Yield 82%; Cream white solid; mp > 250 °C; IR (KBr, cm^{-1}) ν_{max}: 3340 and 3209 (NH_2), 1647 (C=N); ^{1}H NMR (DMSO-d_6, 500 MHz) δ: 12.92 (brs, 1H, NH), 7.76–6.93 (m, 9H, phenyl), 6.78 (brs, 2H, NH_2), 5.80 (s, 1H, H_4), 2.69–2.67 (m, 2H, CH_2), 2.39–2.18 (m, 2H, CH_2), 2.12 (s, 3H, CH_3 phenyl), 1.73–1.70 (m, 4H, $2CH_2$); ^{13}C NMR (DMSO-d_6, 125 MHz) δ: 156.3, 155.0, 152.6, 140.6, 137.6, 135.6, 128.7, 128.4, 127.4, 126.2, 112.4, 99.8, 99.7, 33.0, 28.9, 22.5, 21.3, 21.2, 20.4; Anal. Calcd for $C_{26}H_{24}N_4O$: C, 76.45; H, 5.92; N, 13.72. Found: C, 76.31; H, 5.73; N, 13.61.

5.2.24. 4-(4-Methoxyphenyl)-3-phenyl-2,4,6,7,8,9-hexahydropyrazolo[4′,3′:5,6]pyrano[2,3-b]quinolin-5-amine ***(32)***

Yield 89%; White solid; mp > 250 °C; IR (KBr, cm^{-1}) ν_{max}: 3342 and 3220 (NH_2), 1647 (C=N); ^{1}H NMR (DMSO-d_6, 500 MHz) δ: 12.90 (brs, 1H, NH), 7.74–7.33 (m, 5H, phenyl-pyrazole), 7.23 (d, J = 8.5 Hz, 2H, phenyl), 6.71 (brs, 2H, NH_2), 6.66 (d, J = 8.5 Hz, 2H, phenyl), 5.77 (s, 1H, H_4), 3.57 (s, 3H, OCH_3), 2.64–2.62 (m, 2H, CH_2), 2.36–2.15 (m, 2H, CH_2), 1.68–1.66 (m, 4H, CH_2); ^{13}C NMR (DMSO-d_6, 125 MHz) δ: 158.6, 157.3, 155.1, 152.3, 151.9, 138.4, 136.6, 129.7, 129.6, 129.5, 129.3, 127.1, 114.3, 113.3, 100.9, 100.7, 55.7, 33.5, 30.8, 23.5, 22.3, 22.2; MS (m/z, %): 424 (M^+, 40), 317 (100); Anal. Calcd for $C_{26}H_{24}N_4O_2$: C, 73.56; H, 5.70; N, 13.20. Found: C, 73.67; H, 5.59; N, 13.01.

5.2.25. 3-Phenyl-4-(3,4,5-trimethoxyphenyl)-2,4,6,7,8,9-hexahydropyrazolo[4′,3′:5,6]pyrano[2,3-b]quinolin-5-amine ***(33)***

Yield 79%; White solid; mp > 250 °C; IR (KBr, cm^{-1}) ν_{max}: 3489 and 3400 (NH_2), 1591 (C=N); ^{1}H NMR (DMSO-d_6, 500 MHz) δ: 12.64 (brs, 1H, NH), 7.77 (d, J = 7.8 Hz, 2H, phenyl-pyrazole), 7.47 (d, J = 7.8 Hz, 2H, phenyl-pyrazole), 7.38 (t, J = 7.8 Hz, 1H, phenyl-pyrazole), 6.57 (s, 2H, phenyl), 5.80 (brs, 2H, NH_2), 5.61 (s, 1H, H_4), 3.53 (s, 6H, $2OCH_3$), 3.52 (s, 3H, OCH_3), 2.61–2.58 (m, 2H, CH_2), 2.37–2.22 (m, 2H, CH_2), 1.73–1.69 (m, 4H, $2CH_2$); ^{13}C NMR (DMSO-d_6, 125 MHz) δ: 157.7, 155.1, 152.3, 140.3, 137.3, 135.8, 129.4, 128.7, 128.2, 126.5, 112.0, 105.6, 105.0, 100.1, 98.7, 59.8, 55.9, 55.6, 34.3, 31.7, 23.0, 22.3, 22.1; Anal. Calcd for $C_{28}H_{28}N_4O_4$: C, 69.41; H, 5.82; N, 11.56. Found: C, 69.63; H, 5.97; N, 11.39.

5.2.26. 4-Isopropyl-3-phenyl-2,4,6,7,8,9-hexahydropyrazolo [4′,3′:5,6]pyrano[2,3-b]quinolin-5-amine ***(34)***

Yield 88%; White solid; mp > 250 °C; IR (KBr, cm^{-1}) ν_{max}: 3363 and 3342 (NH_2), 1657 (C=N); ^{1}H NMR (DMSO-d_6, 500 MHz) δ: 12.65 (brs, 1H, NH), 7.74–7.36 (m, 3H, phenyl-pyrazole), 6.52 (brs, 2H, NH_2), 4.67 (s, 1H, H_4), 2.61–2.59 (m, 2H, CH_2), 2.40–2.34 (m, 2H, CH_2), 1.95–1.98 (m, 1H, CH), 1.77–1.72 (m, 4H, $2CH_2$), 0.52 (d, J = 5.5 Hz, 3H, CH_3), 0.38 (d, J = 5.5 Hz, 3H, CH_3); ^{13}C NMR (DMSO-d_6, 125 MHz) δ: 155.3, 153.8, 149.5, 138.4, 130.5, 128.7, 128.2, 126.8, 112.2, 98.9, 96.1, 33.4, 33.0, 30.2, 22.9, 21.8, 20.5, 16.8; MS (m/z, %): 360 (M^+, 8), 317 (100), 77 (45); Anal. Calcd for $C_{22}H_{24}N_4O$: C, 73.31; H, 6.71; N, 15.54. Found: C, 73.42; H, 6.59; N, 15.41.

5.2.27. 1,3,4-Triphenyl-1,4,6,7,8,9-hexahydropyrazolo[4′,3′:5,6] pyrano[2,3-b]quinolin-5-amine ***(35)***

Yield 81%; Cream white solid; mp > 250 °C; IR (KBr, cm^{-1}) ν_{max}: 3455 and 3361 (NH_2), 1595 (C=N); ^{1}H NMR (DMSO-d_6, 500 MHz) δ: 8.01–7.99 (m, 3H, phenyl), 7.35–7.07 (m, 14H, phenyl and NH_2),5.15 (s, 1H, H_4), 3.04–3.03 (m, 4H, $2CH_2$), 1.79–1.77 (m, 4H, $2CH_2$); ^{13}C NMR (DMSO-d_6, 125 MHz) δ: 158.1, 154.5, 149.5, 145.7, 140.8, 135.1, 128.4, 128.0, 127.8, 127.7, 127.4, 126.9, 126.4, 124.9, 123.6, 119.6, 101.5, 44.9, 35.0, 23.7; Anal. Calcd for $C_{31}H_{26}N_4O$: C, 79.12; H, 5.57; N, 11.91. Found: C, 79.32; H, 5.62; N, 11.78.

5.2.28. 3,4-Diphenyl-4,6,7,8,9,10-hexahydro-2H-cyclohepta[b] pyrazolo[4′,3′:5,6]pyrano[3,2-e]pyridin-5-amine ***(36)***

Yield 86%; White solid; mp > 250 °C; IR (KBr, cm^{-1}) ν_{max}: 3355 and 3204 (NH_2), 1639 (C=N); ^{1}H NMR (DMSO-d_6, 500 MHz) δ: 13.14 (brs, 1H, NH), 7.76 (d, J = 7.0 Hz, 2H, phenyl-pyrazole), 7.63 (brs, 2H, NH_2), 7.47 (t, J = 7.0 Hz, 2H, phenyl-pyrazole),7.41 (t, J = 7.0 Hz, 1H, phenyl-pyrazole), 7.34 (d, J = 7.5 Hz, 2H, phenyl), 7.15 (t, J = 7.0 Hz, 2H, phenyl), 7.08 (t, J = 6.5 Hz, 1H, phenyl), 5.97 (s, 1H, H_4), 2.97–2.95 (m, 2H, CH_2), 2.75–2.64 (m, 2H), 2.38–1.73 (m, 6H, $3CH_2$); ^{13}C NMR (DMSO-d_6, 125 MHz) δ: 156.5, 150.3, 142.6, 138.4, 128.8, 128.3, 127.6, 126.9, 126.5, 118.2, 100.4, 99.2, 33.2, 31.5, 30.9, 25.5, 24.8, 24.0; Anal. Calcd for $C_{26}H_{24}N_4O$: C, 76.45; H, 5.92; N, 13.72. Found: C, 76.52; H, 5.81; N, 13.79.

5.2.29. 4-(4-Chlorophenyl)-3-phenyl-4,6,7,8,9,10-hexahydro-2H-cyclohepta[b]pyrazolo[4′,3′:5,6]pyrano[3,2-e]pyridin-5-amine ***(37)***

Yield 81%; White solid; mp > 250 °C; IR (KBr, cm^{-1}) ν_{max}: 3351 and 3202 (NH_2), 1635 (C=N); ^{1}H NMR (DMSO-d_6, 500 MHz) δ: 13.10 (brs, 1H, NH), 7.70–7.69 (m, 2H, phenyl-pyrazole), 7.56 (brs, 2H, NH_2), 7.43 (d, J = 7.3 Hz, 2H, phenyl-pyrazole), 7.37 (t, J = 7.3 Hz, 1H, phenyl-pyrazole), 7.32 (d, J = 8.5 Hz, 2H, phenyl), 7.16 (d, J = 8.5 Hz, 2H, phenyl), 5.96 (s, 1H, H_4), 2.92–2.91 (m, 2H, CH_2), 2.68–2.46 (m, 2H, CH_2), 1.80–1.33 (m, 6H, $3CH_2$); ^{13}C NMR (DMSO-d_6, 125 MHz) δ: 157.3, 155.7, 152.9, 151.2, 142.4, 139.3, 132.4, 130.3, 129.7, 129.2, 129.1, 127.4, 119.2, 100.8, 99.5, 33.5, 32.5, 31.7, 26.3, 25.7, 24.9; MS (m/z, %): 442 (M^+, 61), 444 (M+2, 23), 390 (13), 331 (100), 246 (17); Anal. Calcd for $C_{26}H_{23}ClN_4O$: C, 70.50; H, 5.23; N, 12.65. Found: C, 70.22; H, 5.11; N, 12.39.

5.2.30. 4-(4-Chlorophenyl)-3-phenyl-4,6,8,9-tetrahydro-2H-pyrazolo[4′,3′:5,6]pyrano[2,3-b]thiopyrano[3,4-e]pyridin-5-amine ***(38)***

Yield 77%; White solid; mp > 250 °C; IR (KBr, cm^{-1}) ν_{max}: 3431 and 3376 (NH_2), 1647 (C=N); ^{1}H NMR (DMSO-d_6, 500 MHz) δ: 13.19 (brs, 1H, NH), 7.78–7.76 (m, 4H, phenyl), 7.43–7.39 (m, 4H, phenyl and NH_2), 7.34 (t, J = 7.3 Hz, 1H, phenyl), 7.16 (d, J = 8.5 Hz, 2H, phenyl), 6.12 (s, 1H, H_4), 3.56–3.32 (m, 2H, CH_2), 3.09–2.99 (m, 2H, CH_2), 2.86 (s, 2H, CH_2); ^{13}C NMR (DMSO-d_6, 125 MHz) δ: 156.9, 155.7, 152.1, 146.6, 142.4, 139.2, 132.4, 130.4, 129.6, 129.1, 127.3, 112.1, 100.4, 99.5, 33.3, 29.8, 23.7, 23.6; MS (m/z, %): 446 (M^+, 12), 448 (M+2, 4), 335 (78), 289 (13); Anal. Calcd for $C_{24}H_{19}ClN_4OS$: C, 64.49; H, 4.28; N, 12.54. Found: C, 64.31; H, 4.17; N, 12.71.

5.2.31. 3-(Furan-2-yl)-4-phenyl-2,4,6,7,8,9-hexahydropyrazolo [4′,3′:5,6]pyrano[2,3-b]quinolin-5-amine ***(39)***

Yield 90%; Cream solid; mp > 250 °C; IR (KBr, cm^{-1}) ν_{max}: 3464 and 3338 (NH_2), 1596 (C=N); ^{1}H NMR (DMSO-d_6, 500 MHz) δ: 12.76 (brs, 1H, NH), 7.71–7.70 (m, 1H, furyl), 7.34–7.32 (m, 2H, phenyl), 7.12–7.10 (m, 2H, phenyl), 7.01–6.99 (m, 1H, phenyl), 6.88–6.86 (m, 1H, furyl), 6.58–6.57 (m, 1H, furyl), 5.66 (brs, 2H, NH_2), 5.48 (s, 1H, H_4), 3.14–3.12 (m, 2H, CH_2), 2.30–2.15 (m, 2H, CH_2), 1.66–1.64 (m, 4H, $2CH_2$); ^{13}C NMR (DMSO-d_6, 125 MHz) δ: 153.5, 152.9, 145.5, 143.7, 128.8, 128.6, 127.0, 113.1, 112.6, 108.6, 100.1, 49.4, 34.6, 32.8, 23.8, 23.2, 22.9; MS (m/z, %): 384 (M^+, 28), 307 (100), 283 (47); Anal. Calcd for $C_{23}H_{20}N_4O_2$: C, 71.86; H, 5.24; N, 14.57. Found: C, 71.95; H, 5.46; N, 14.32.

*5.2.32. 3-(Furan-2-yl)-1,4-diphenyl-1,4,6,7,8,9-hexahydropyrazolo [4′,3′:5,6]pyrano[2,3-b]quinolin-5-amine **(40)***

Yield 83%; Cream solid; mp > 250 °C; IR (KBr, cm^{-1}) ν_{max}: 3475 and 3261 (NH_2), 1644 (C=N); ^1H NMR (DMSO-d_6, 500 MHz) δ: 7.87–7.86 (m, 2H, phenyl), 7.71–7.70 (m, 1H, furyl), 7.54–7.52 (m, 2H, phenyl), 7.43–7.42 (m, 2H, phenyl), 7.35–7.33 (m, 1H, phenyl), 7.16–7.14 (m, 2H, phenyl), 7.06–7.04 (m, 1H, phenyl), 6.94–6.92 (m, 1H, furyl), 6.59–6.57 (m, 1H, furyl), 5.87 (brs, 2H, NH_2), 5.60 (s, 1H, H_4), 2.57–2.55 (m, 2H, CH_2), 2.34–2.16 (m, 2H, CH_2), 1.67–1.65 (m, 4H, $2CH_2$); ^{13}C NMR (DMSO-d_6, 125 MHz) δ: 154.9, 153.4, 153.2, 148.1, 147.8, 144.8, 143.6, 139.8, 138.5, 130.3, 128.9, 127.5, 127.3, 121.5, 114.3, 112.4, 109.4, 100.3, 99.8, 35.2, 32.7, 23.9, 23.1, 22.8; MS (*m*/*z*, %): 460 (M^+, 44), 383 (91), 355 (7); Anal. Calcd for $C_{29}H_{24}N_4O_2$: C, 75.63; H, 5.25; N, 12.17. Found: C, 75.72; H, 5.17; N, 12.42.

5.3. Cholinesterases inhibition assay

Acetylcholinesterase from *Electrophorus electricus* (electric eel, type V-s, lyophilized powder, ≥1000 units/mg protein), human butyrylcholinesterase (recombinant, expressed in goat, ≥500 units/mg protein), acetylthiocholine iodide, butyrylthiocholine iodide, 5,5′-dithiobis[2-nitrobenzoic acid] (DTNB), and tacrine were purchased from Sigma-Aldrich. The AChE and BuChE inhibitory activity of target compounds was evaluated by Ellman's method as reported earlier [24,25]. In brief, the test compounds were dissolved in the solvent system ethanol/DMSO (9:1, 1 mL) and then diluted using phosphate buffer to achieve assay concentrations. The assay mixture comprised of 2000 μL phosphate buffer (0.1 M, pH = 8.0), 65 μL of DTNB 0.1 M, 35 μL of enzyme (0.2 U/ml) and 50 μL of inhibitor. The mixture was incubated for 5 min at room temperature. Afterward, 10 μL of substrate (acetylthiocholine iodide, 0.01 M) was added and the change of the absorbance was measured at 412 nm for 1 min. The same protocol was applied for determination of BuChE activity by using butyrylthiocholine iodide as substrate. All experiments were performed on a Synergy HTX Multi-Mode Reader-BioTek.

5.4. 15-LOX inhibition assay

The 15-LOX inhibitory activity of compounds **9**–**40** was determined by using soybean lipoxygenase enzyme (type 1-B lyophilized powder ≥50000 units/mg solid, Sigma) as reported previously [26,27]. In this test, the conversion of linoleic acid to 13-hydroperoxylinoleic acid by 15-LOX enzyme was measured spectrophotometrically at 234 nm. Quercetin was used as a standard inhibitor. Briefly, the tested compounds were dissolved in DMSO (1 mL) and then diluted in phosphate buffer (0.1 M, pH = 8) as needed. 50 μL of the test compounds was added to the test solution containing 50 μL of enzyme (final concentration: 167 U/ml) and 3000 μL phosphate buffer (0.1 M, pH = 8). After 5 min incubation at room temperature, 10 μL substrate (linoleic acid in ethanol, final concentration: 134 mM) was added and the change in the absorbance was read for 1 min at 234 nm. All experiments were performed on Unico double beam spectrophotometer.

5.5. In vitro cytotoxicity assay against HepG2 cell line

The human hepatocellular carcinoma cell line (HepG2) was purchased from Iranian Biological Resource Center (IBRC), Tehran, Iran. The cells were cultured in DMEM medium supplemented with 10% FBS at 37 °C in a humidified atmosphere of 5% CO_2 and 95% air. To determine the cytotoxic effect of the test compounds, the HepG2 cells were harvested in the exponential phase of growth and sub-cultured in 96-well tissue culture microplate at a seeding density of 15000 cells per well and allowed to adhere for 24 h. Thereafter, the medium was replaced by fresh medium containing desired concentrations (1–500 μM) of each tested compound (**29**, **32**, and **40**) and incubated for 24 h. Consequently, the medium was removed and 20 μL of DMEM medium containing MTT (5 mg/mL) was added to each well. After incubation for 4 h, followed by replacement of medium with 100 μL of DMSO, the optical density was measured at 540 nm. All mentioned procedures were performed in triplicate and the obtained results were used for determination of viability percent with respect to the control group.

Acknowledgments

This research has been supported by grants from the Research Council of Tehran University of Medical Sciences (Grant no. 29594-181-02-94) and Iran National Science Foundation (INSF) (Grant no. 92037263).

Appendix A. Supplementary data

Supplementary data related to this article can be found at http://dx.doi.org/10.1016/j.ejmech.2016.07.043.

References

[1] N. Guzior, A. Więckowska, D. Panek, B. Malawska, Curr. Med. Chem. 22 (2015) 373–404.
[2] Alzheimer's Disease International, World Alzheimer Report, 2011, p. 1.
[3] C. Reitz, R. Mayeux, Biochem. Pharmacol. 88 (2014) 640–651.
[4] E. Mikiciuk-Olasik, P. Szymański, E. Żurek, Ind. J. Exp. Biol. 45 (2007) 315–325.
[5] H.W. Querfurth, F.M. LaFerla, N. Engl. J. Med. 362 (2010) 329–344.
[6] R.T. Bartus, R.L. Dean, B. Beer, A.S. Lippa, Science 217 (1982) 408–417.
[7] E. Scarpini, P. Scheltens, H. Feldman, Lancet Neurol. 2 (2003) 539–547.
[8] J. Birks, Cochrane Database Syst. Rev. 1 (2006) CD005593.
[9] D. Praticò, V. Zhukareva, Y. Yao, K. Uryu, C.D. Funk, J.A. Lawson, J.Q. Trojanowski, V.M. Lee, Am. J. Pathol. 164 (2004) 1655–1662.
[10] Y.B. Joshi, P.F. Giannopoulos, D. Praticò, Trends Pharmacol. Sci. 36 (2015) 181–186.
[11] T. Schewe, Biol. Chem. 383 (2002) 365–374.
[12] A.R. Brash, J. Biol. Chem. 274 (1999) 23679–23682.
[13] G.W. Small, JAMA 268 (1992) 2564–2565.
[14] P.B. Watkins, H.J. Zimmerman, M.J. Knapp, S.I. Gracon, K.W. Lewis, JAMA 271 (1994) 992–998.
[15] M. Khoobi, M. Alipour, A. Moradi, A. Sakhteman, H. Nadri, S.F. Razavi, M. Ghandi, A. Foroumadi, A. Shafiee, Eur. J. Med. Chem. 68 (2013) 291–300.
[16] D. Silva, M. Chioua, A. Samadi, M. Carmo Carreiras, M.L. Jimeno, E. Mendes, L. Ríos Cde, A. Romero, M. Villarroya, M.G. López, J. Marco-Contelles, J. Eur. J. Med. Chem. 46 (2011) 4676–4681.
[17] E. Maalej, F. Chabchoub, M.J. Oset-Gasque, M. Esquivias-Pérez, M.P. González, L. Monjas, C. Pérez, C. de los Ríos, M.I. Rodríguez-Franco, I. Iriepa, I. Moraleda, M. Chioua, A. Romero, J. Marco-Contelles, A. Samadi, Eur. J. Med. Chem. 54 (2012) 750–763.
[18] E. Maalej, F. Chabchoub, A. Samadi, C. De los Rios, A. Perona, A. Morreale, J. Marco-Contelles, Bioorg. Med. Chem. Lett. 21 (2011) 2384–2388.
[19] S.S. Xie, X. Wang, N. Jiang, W. Yu, K.D.G. Wang, J.S. Lan, Z.-R. Li, L.Y. Kong, Eur. J. Med. Chem. 95 (2015) 153–165.
[20] S.S. Xie, J.S. Lan, X.B. Wang, N. Jiang, G. Dong, Z.R. Li, K.D.G. Wang, P.P. Guo, L.Y. Kong, Eur. J. Med. Chem. 93 (2015) 42–50.
[21] M. Khoobi, F. Ghanoni, H. Nadri, A. Moradi, M. Pirali Hamedani, F. Homayouni Moghadam, S. Emami, M. Vosooghi, R. Zadmard, A. Foroumadi, A. Shafiee, Eur. J. Med. Chem. 89 (2015) 296–303.
[22] F. Cheng, W. Li, Y. Zhou, J. Shen, Z. Wu, G. Liu, P.W. Lee, Y. Tang, J. Chem. Inf. Model 52 (2012) 3099–3105.
[23] D.E. Clark, Comb. Chem. High. Throughput Screen. 4 (2001) 477–496.
[24] G.L. Ellman, K.D. Courtney, V. Andresjr, R.M. Featherstone, Biochem. Pharmacol. 7 (1961) 88–95.
[25] S. Mohammad Bagheri, M. Khoobi, H. Nadri, A. Moradi, S. Emami, L. Jalili-Baleh, F. Jafarpour, F. Homayouni Moghadam, A. Foroumadi, A. Shafiee, Chem. Biol. Drug Des. 86 (2015) 1215–1220.
[26] K.E. Malterud, K.M. Rydland, J. Agric. Food Chem. 48 (2000) 5576–5580.
[27] M. Barazandeh Tehrani, S. Emami, M. Asadi, M. Saeedi, M. Mirzahekmati, S.M. Ebrahimi, M. Mahdavi, H. Nadri, A. Moradi, F. Homayouni Moghadam, S. Farzipour, M. Vosooghi, A. Foroumadi, A. Shafiee, Eur. J. Med. Chem. 87 (2014) 759–764.